

48476852
99 C 1025

MEMORANDUM FOR PRS (In-House / Contractor Publication)

FROM: PROI (STINFO)

13 June 2002

SUBJECT: Authorization for Release of Technical Information, Control Number: **AFRL-PR-ED-TP-2002-145**
Mke Fife (PRSS) et al., "The Development of a Flexible, Usable Plasma Interaction Modeling System"

38th AIAA/ASME/SAE/ASEE JPC&E
(Indianapolis, IN, 7-10 July 2002) (Deadline = 07 July 2002)

(Statement A)

1. This request has been reviewed by the Foreign Disclosure Office for: a.) appropriateness of distribution statement, b.) military/national critical technology, c.) export controls or distribution restrictions, d.) appropriateness for release to a foreign nation, and e.) technical sensitivity and/or economic sensitivity.

Comments: _____

Signature _____ Date _____

2. This request has been reviewed by the Public Affairs Office for: a.) appropriateness for public release and/or b) possible higher headquarters review.

Comments: _____

Signature _____ Date _____

3. This request has been reviewed by the STINFO for: a.) changes if approved as amended, b) appropriateness of references, if applicable; and c.) format and completion of meeting clearance form if required

Comments: _____

Signature _____ Date _____

4. This request has been reviewed by PR for: a.) technical accuracy, b.) appropriateness for audience, c.) appropriateness of distribution statement, d.) technical sensitivity and economic sensitivity, e.) military/national critical technology, and f.) data rights and patentability

Comments: _____

APPROVED/APPROVED AS AMENDED/DISAPPROVED

PHILIP A. KESSEL Date
Technical Advisor
Space and Missile Propulsion Division

The Development of a Flexible, Usable Plasma Interaction Modeling System

J. M. Fife and M. R. Gibbons
U.S. Air Force Research Laboratory
Edwards AFB, CA

D. B. VanGilder and D. E. Kirtley
ERC, Inc.
Edwards AFB, CA

A 3-D computational plasma interaction modeling system is being developed to predict the interaction of electric propulsion plumes with surfaces. The system, named COLISEUM, is designed to be flexible, usable, and expandable, allowing users to define surfaces with their choice of off-the-shelf 3-D solid modeling packages. These surfaces are then loaded into COLISEUM, which performs plasma operations based on user commands. Functional modules are interchangeable, and can range from simple (prescribed plume field) to complex (PIC-DSMC). Surface interaction parameters such as ion flux, ion energy, sputtering, and re-deposition are computed. Development to date has progressed to include the two simplest functional modules: *prescribed plume*, which imports and superimposes a plume distribution, and *ray*, which performs ray tracing of flux from point sources. This paper presents a new COLISEUM algorithm for calculating equilibrium re-sputtering and re-deposition of materials. This algorithm enables calculation of net deposition and sputtering of surfaces inside HET test facilities as well as in the space environment. Two cases are presented – one for a laboratory experiment in which sputtering and redeposition were measured, and another in which sputtering and redeposition on a generalized geosynchronous spacecraft is predicted.

Introduction

Onboard electric propulsion (EP) thrusters, which use electric power to generate or augment thrust, hold the promise of greatly increased satellite maneuverability, and enabling new missions. Many types of EP thrusters are already in mature states of development, and many can achieve specific impulses over 3000 seconds. This, combined with growing electric power levels onboard new-generation spacecraft, is pushing EP rapidly into the mainstream.^{1,2}

Several EP devices are currently being evaluated for use onboard U.S. commercial and military spacecraft. One of the most promising for near-term use is the Hall-effect thruster (HET). Over 120 HETs have flown on Russian spacecraft, where typical flight units have specific impulses around 1600 seconds and efficiencies near 50%.³ HETs operate by generating a stationary xenon plasma inside an annular channel. Strong radial magnetic fields are applied which impede electron motion, but allow ions to accelerate axially out of the device with velocities around 20 km/s (energies of around 300 eV).

High-energy HET exhaust ions may erode (sputter) surfaces on which they impinge. In addition, this sputtered material may be re-deposited on other spacecraft surfaces. These issues, and others, such as electromagnetic interference and spacecraft charging, cause some concern for spacecraft designers who want the maneuverability EP offers but do not want increased risk.

Efforts are underway to quantify some of the risks associated with integration of EP with spacecraft, including surface erosion and re-deposition. Work has been done to computationally model expansion of HET plumes.⁴ Additionally, Gardner et al. have developed Environment Work Bench (EWB), a code that calculates sputtering of spacecraft surfaces by superimposing pre-computed EP plumes onto spacecraft geometries.^{5,6} However, existing codes do not self-consistently calculate the plume expansion with 3-D surface sputtering in a usable, flexible way.

The Air Force Research Laboratory is leading development of a new software package named COLISEUM, which is capable of self-consistently modeling plasma propagation and interactions with arbitrary 3-D surfaces. Three important requirements have been placed on COLISEUM: It must be **USABLE**, **FLEXIBLE**, and **EXPANDABLE**.

USABLE means a typical engineer should be able to set up and run a typical low-fidelity case in less than one day with less than three days training.

FLEXIBLE means COLISEUM must be able to simulate at least three important cases: a) a single spacecraft, b) multiple spacecraft in formation, and c) laboratory conditions (e.g. the interior of a vacuum test facility). Simulating laboratory conditions is very important for two reasons. First, since there is very little on-orbit data for EP thrusters, ground-based tests must be relied upon for the bulk of code validation.

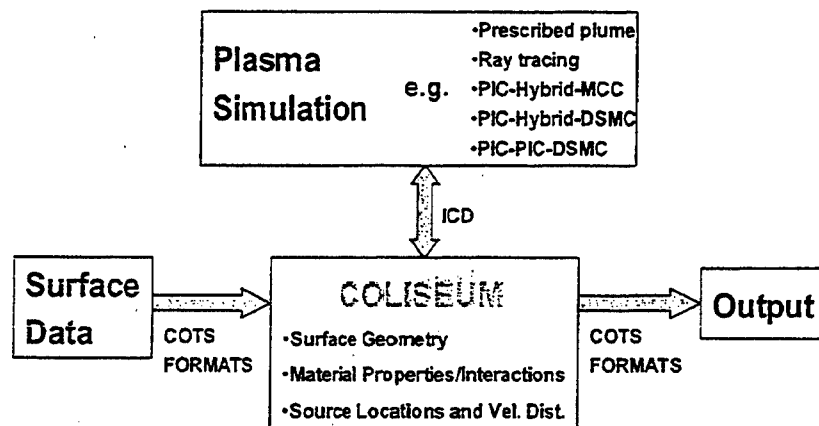


Fig. 1 Architecture for using various interchangeable plasma simulation techniques with the same 3-D surface geometry.

Second, by modeling the laboratory conditions, COLISEUM can help engineers interpret lab measurements.

In addition to being able to simulate multiple geometries, COLISEUM must be flexible in its use of plasma simulation algorithms. It must be able to use a variety of interchangeable plasma simulation algorithms for each geometry. Therefore, if low run-time is desired, a low-fidelity technique can be selected such as ray tracing. For higher fidelity (at the cost of longer run-time), something like Particle-In-Cell (PIC) can be used.

EXPANDABLE means COLISEUM can be easily expanded to incorporate new plasma simulation algorithms, new capabilities, or improved efficiency. Furthermore, as new plasma simulation algorithms are added, old ones must continue to work.

Approach

Fig. 1 shows how COLISEUM integrates surface geometries with a suite of various interchangeable plasma simulations. In general, COLISEUM can be viewed as a toolbox or framework in which 3-D plasma simulations can be quickly integrated. Common calculations (such as those related to surfaces, material properties, and flux sources) are standardized and provided as resources (data and subroutines) to each simulation.

From a code architecture standpoint, COLISEUM has been designed as a collection of modules, each with a specific function and hierarchy. Each module contains data and associated code. Modules may be categorized into three levels.

Level 0 modules perform functions related to user-interaction. Although COLISEUM is fundamentally command-driven, a Graphical User Interface (GUI) front end is envisioned for the future.

Level 1 modules are the primary components of COLISEUM. They calculate plasma propagation on the volume domain. They contain algorithms, such as fluid, PIC, DSMC, or hybrids thereof, which perform a solution subject to pre-set boundary conditions. Level 1 modules are uniform and interchangeable. They all conform to a specific Interface Control Document (ICD) – they have specific inputs, outputs, and resources available to them.

Level 2 modules perform support tasks common to all types of plasma simulations. They handle boundary conditions, and provide support to Level 1 modules. They act as a toolbox or collection of resources.

The purpose of the modular design is to give COLISEUM flexibility and expandability. A large number of Level 1 modules are desired to allow flexibility in solving a variety of different problems. The ICD is, therefore, very important, because it describes for authors of Level 1 modules a) what inputs and boundary conditions must be recognized, b) what outputs are expected, and c) what Level 2 resources are available. The ICD may be distributed to outside groups so that COLISEUM can be expanded through addition of new Level 1 modules.

Surfaces

Surfaces are modeled in finite-element fashion as contiguous triangular elements joined at the vertices (nodes). COLISEUM does not generate 3-D geometries or surfaces; instead, it imports them from other software.

Users create custom geometries using almost any mainstream commercial 3-D solid modeling package. Then, they use finite element analysis software to mesh the surface of their geometry as if they were going to perform a structural analysis using thin shells. The user then saves the meshed surface file in ANSYS format, which is readable by COLISEUM. ANSYS finite element format was chosen because it is widely supported by finite element packages.

Table 1 Sputter yield coefficients for bombardment by singly ionized xenon

Material	Model	C_1	C_2
Al	Roussel	1.0	1.9e16
ITO	Roussel	0.1	6.25e15
Kapton	Roussel	0.001	2.7e13
AgT5	Roussel	1.0	1.9e16
Graphite	Roussel	0.0	1.67e15
Stainless	Roussel	0.0	4.05e15

This concept of separating the surface geometry definition from the plasma calculation has proven very successful. It greatly reduced development time and cost by eliminating the need for a separate surface definition module. It allows users to choose which software to use in defining geometries. And, users can import into COLISEUM geometries that have already been defined for other reasons (structural, thermal, etc.).

Material Properties

The user constructs a database of materials that is read by COLISEUM. The database contains material names, material reference numbers, and molecular weights and charges (in the case of ions). Materials in the database are connected to the surface geometry by the material reference number. Users mark surface materials during geometry/surface definition using their finite element software. They simply set the elastic modulus of the surface component to be equal to the material reference number. This value appears in the ANSYS file, where COLISEUM reads it.

The user also provides a second database, a materials interaction database. This database contains the sputter yield coefficients and sticking coefficients of one material interacting with the other. For example, one important interaction may be between Xe^+ and Kapton.

Sources

Sources are modeled as having a specific velocity distribution that is constant over individual surface elements. A collection of Level 2 commands allows the user to either specify one of a set of source types (mono-energetic, half-Maxwellian, etc.) or read in a file containing a custom discretized velocity distribution function.

Source elements are identified with a source reference number during geometry/surface definitions, much like the materials are identified.

This method is extremely descriptive and general. Level 1 modules may treat this information in various ways. For instance, a Level 1 module could be written to treat the source element a single point source for ray tracing purposes. Alternately, particle methods could sample from the velocity distribution and introduce particles randomly over the full element surface. Therefore, this choice of source definition methods gives COLISEUM great flexibility.

Plasma Simulation

Currently, two Level 1 modules have been written. The first, PRESCRIBED_PLUME, allows the user to import a previously calculated or measured plume field. This plume is superimposed over the user's surface geometry. Plasma densities, fluxes, and sputter rates are then calculated at each surface node.

The second module, RAY, uses ray tracing to calculate the flux from all sources onto all surface nodes. Once again, density, flux, and sputter rate are calculated.

Future modules will incorporate statistical kinetic methods for plasma calculation such as PIC and DSMC. Plans also include development of kinetic algorithms for use on unstructured meshes, adaptive meshes, and domain decomposition. Primarily, these techniques will be incorporated to add flexibility to the simulation. For instance, domain decomposition will allow the domain to be broken into smaller sub-domains, each potentially having different algorithms, depending on local parameters as the Debye length or mean free path.

Sputtering and Redeposition

The material interaction database can support multiple surface sputtering models. Currently, three models are implemented: a) constant yield, b) a model by Roussel et al.⁷ (also used by Gardner et al.⁵), and c) a model by Kannenberg⁸ (REF). The model by Roussel et al., which is used to obtain the results in this paper, is:

$$Y(E, \theta) = (C_1 + C_2 E)(1.0 - 0.72\theta + 11.72\theta^2 - 3.13\theta^3 - 2.57\theta^4) \quad (1)$$

Above, E is the particle energy (in eV) and θ is the off-normal incidence angle (in radians). Table 1 gives the coefficients for the materials used here, indium titanium oxide (ITO), aluminum, silver with Teflon coating, Kapton. ITO is commonly used as an anti-reflective coating on solar array cover glass. Fig. 10 plots sputter yield at $E=300$ eV for several of the materials used here.

For the two existing plasma simulations, PRESCRIBED_PLUME and RAY, redeposition is calculated by ray tracing. The sputtered flux is distributed as the cosine of the off-normal angle and projected from the sputtering elements to all other viewable surface elements. More detailed models will replace this simple model in the future.

Sputtered material may be deposited on surfaces exposed to the ion beam. There, the deposited material may be re-sputtered onto other surfaces, as shown in Fig. 3. This re-sputtering process may be very important because, for certain geometries, it may influence the type and thickness of re-deposited material on a large percentage of the surface.

For the two existing plasma simulations, PRESCRIBED_PLUME and RAY, an algorithm has been developed to model re-sputtering, and iteratively calculate net sputtering and deposition rates at all surface nodes. Fig. 2 shows a flow description of the algorithm.

The algorithm starts by zeroing the total deposition rate of all materials to all nodes. Then, it calculates the new total deposition rate at each node for each material type. On the second and subsequent iteration, the algorithm again calculates the new total deposition rate, but takes into account the deposition from the previous iteration. This process is repeated until equilibrium, defined as the mean residual of the net deposition rate reaching some maximum value.

Deposition from the previous iteration is taken into account by first storing the total deposition rate from the last iteration into a "net" deposition rate variable. As the various sputtering sources (such as ion beams) are considered, this net deposition rate is successively depleted. If and when the net deposition rate becomes zero at a given node, the algorithm begins depleting the native material.

By "depleting", what is meant is that the surface deposition rate is decreased (or native material sputter rate is increased), and this material is projected to all other nodes as deposition (in the case of native material sputtering) or redeposition (in the case of deposited material). When material is projected to all other nodes, the total deposition rate is increased by the appropriate amount in accordance with the cosine sputtering law mentioned earlier.

One key assumption is that the sputter yield of the "composite" deposition material, which may be made up of

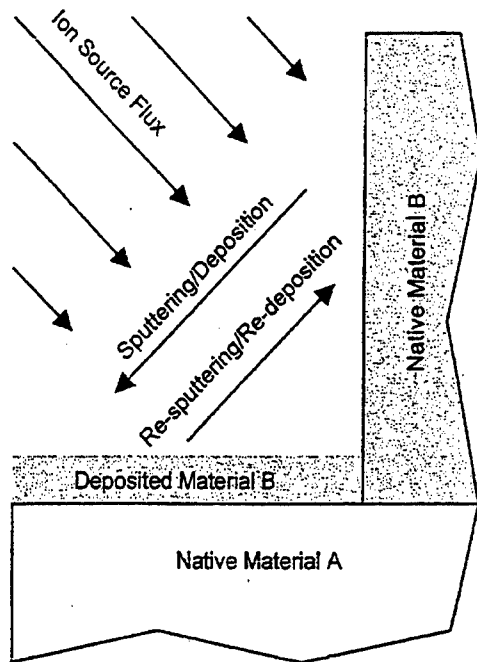


Fig. 3. Illustration of sputtering, deposition, re-sputtering, and re-deposition for a simple geometry with two materials: material A and B, where material B has higher sputter yield than material A.

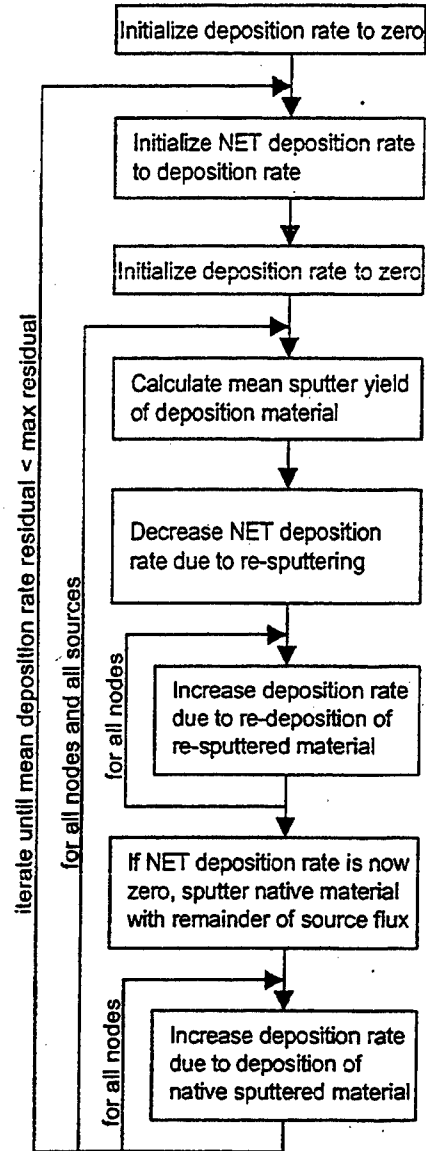


Fig. 2. Flow diagram for re-sputtering algorithm.

many different materials, is the mean of the arriving material sputter yields, weighted by their fluxes:

$$\bar{Y} = \frac{\sum_k Y_k \Gamma_{D,k}}{\sum_k \Gamma_{D,k}} \quad (2)$$

Where Y is the sputter yield, and Γ_D is the normal component of the deposition flux, and k is the index of the arriving material. When re-sputtering the deposited material, the above assumption requires that the re-sputtered flux of each material be:

```

# coliseum.in
#
# Load a GEO satellite geometry,
# add a 3kW HET source, calculate
# the flux and sputtering using
# ray tracing, and save the
# results in Tecplot format.
#

material_load material.txt mat_mat.txt

surface_load ANSYS GEO_Sat.ANS

source_specify 18 FLUX_PHI 0007 het_3kw.dat
12e-6 16000.0 1.0

ray DEPOSIT 5

surface_save TECPLOT GEO_Sat.dat
FLUXNORMAL.XE+ SPUTTERRATE

```

Fig. 4. Sample COLISEUM command file

$$\Gamma_{R,k} = \bar{\Gamma}_S \frac{\Gamma_{D,k}}{\sum_k \Gamma_{D,k}} \quad (3)$$

Where Γ_S is the flux of source particles normal to the surface. This ensures material conservation and preserves the ratio of constituents of the composite deposition material.

User Interface

The user enters commands via a COLISEUM input file. The commands are executed sequentially as they appear in the input file. Each command may have some number of parameters separated by spaces or commas. A sample input file is shown in Fig. 4.

Typical run times for low-fidelity cases (using PRESCRIBED_PLUME or RAY) take approximately 20 seconds on a 2 GHz Intel Pentium 4 workstation. Once more detailed physics are incorporated, with Level 1 modules incorporating such algorithms as PIC-DSMC, run times are expected to be between 20 minutes and 20 hours, depending on the level of fidelity and on the initial conditions.

Results and Discussion

For the results presented here, COLISEUM, runs were executed for two cases: a) an HET firing inside a laboratory vacuum chamber, and b) a fictitious geosynchronous satellite with an HET firing in the north direction (as if for stationkeeping). Case a) is an attempt to validate the sputtering models, and case b) is a generalized application to a fictitious spacecraft problem. In both cases, the simple plasma simulation module, PRESCRIBED_PLUME, was used to incorporate a previously calculated plume expansion model onto the surface geometry. The plume expansion model used here was calculated for a Busek 200-Watt HET⁹ by SAIC using the GILBERT⁵ toolbox. Comparisons of this

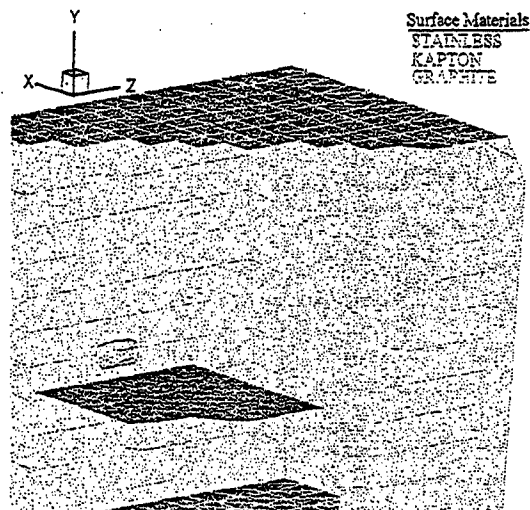


Fig. 6. Cutaway of an HET test setup showing the HET, a horizontal Kapton-covered table, graphite panels, and some exposed stainless steel vacuum chamber wall.

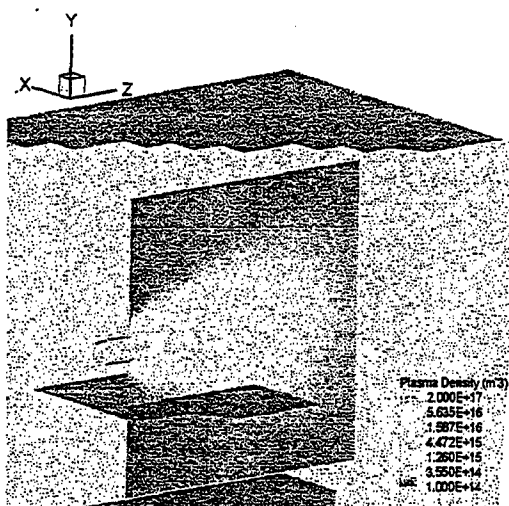


Fig. 5. Slice showing plasma density from a 200-Watt HET firing inside the test setup.

plume model with experiment can be found in a paper by Gardner et al.¹⁰

Results from case a) are shown in Fig. 6 through Fig. 9. Fig. 6 shows the geometry of a test performed at AFRL. Inside a vacuum chamber, the Busek 200W engine was mounted horizontally on the chamber centerline. A horizontal aluminum table covered with Kapton was mounted 0.188m below the engine. Samples of Kapton 1 cm² were placed on center of the table at varying distances from the thruster exit plane. Graphite panels were placed around the experiment and on the vacuum chamber door to form a shroud around the plume and reduce sputtering.

The Kapton samples were measured and weighed before and after a 100-hour engine firing at (OPERATING CONDITIONS). The difference in sample masses was recorded, and agreed well with the difference in sample thickness.

The 3-D chamber model is broken down into triangular elements. Two commercial packages, SolidWorks and COSMOS/DesignStar, were used to generate these surface geometries. Final plotting was performed by another commercially available package, Tecplot. The colors of the mesh lines indicate the type of material.

Fig. 5 shows a slice through the 200-Watt HET plume superimposed on the model. Plasma density is highest near the HET exhaust, and drops off rapidly as the plume expands into the test section.

Fig. 7 shows the convergence properties of the re-sputtering algorithm presented in the previous section. As can be seen from the figure, the mean residual of the net deposition rate decreases exponentially with the number of iterations. For geometries with around 2000 surface elements, convergence to zero residual (machine precision) typically occurs after approximately 30 iterations.

Fig. 8 and Fig. 9 show the resulting net sputtering and deposition, respectively. The net sputtering peaks on the Kapton-covered table where the incidence angle of the ion beam is approximately 60 degrees. This is due to two effects – increased xenon ion flux at that point, and the model for Kapton sputtering yield, which also peaks at approximately 60 degrees. The net graphite deposition rate (shown viewed from downstream of the thruster plume) peaks underneath the Kapton-covered table, where plume impingement is blocked by the table. In most other regions, deposited graphite is “cleaned” from the surfaces by the plume, resulting in much lower graphite deposition rates in those areas.

Fig. 10 compares the measured and calculated values of Kapton sputtering/redeposition. Two calculated values are shown – one in which redeposition is not considered, and another with redeposition.

Negative values indicate net deposition of Graphite that was sputtered from the panels. Net deposition can be seen for $z < 1\text{m}$ in the measurements, and $z < 0\text{m}$ in the calculation. This area is underneath the HET, and behind the plume impingement region. Therefore, very little ion flux exists to sputter away re-deposited graphite.

Comparing the two calculated results in Fig. 10, one can see the effect of redeposition on the net sputtering rate. For this geometry, redeposition lowers the net sputtering rate by around 2%. This is due to the fact that ions must now sputter graphite deposition before sputtering the native Kapton. This results in a lower net sputtering rate of Kapton. Ion sputtering dominates on the Kapton-covered table. In areas where the

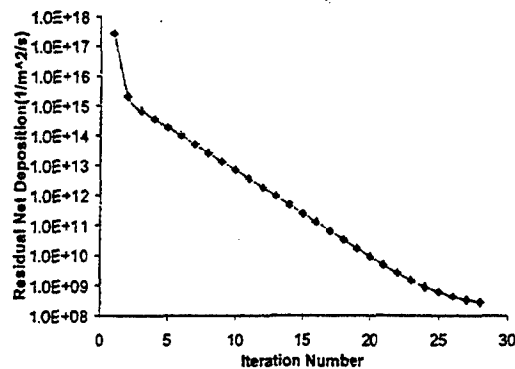


Fig. 7. Convergence of the residual of the mean net deposition rate versus iteration number for the laboratory test case.

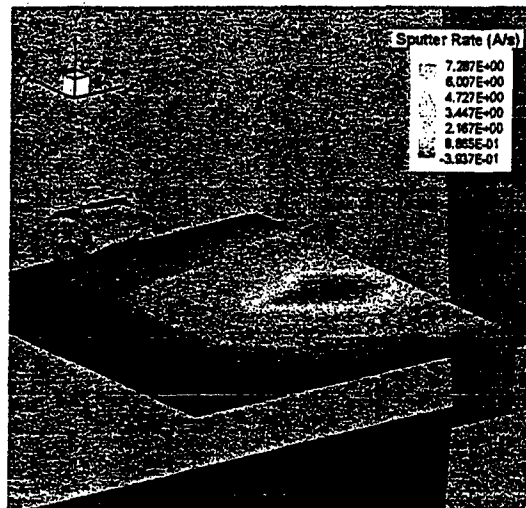


Fig. 8. Net surface sputtering rate.

ion beam flux is lower, re-sputtering will have a greater influence.

Also in Fig. 10, one can see that the measured and calculated net sputtering rate of Kapton differ by a factor of ~4. Some possible explanations are: a) our model for Kapton sputtering is high by a factor of ~4, b) the 200W HET plume model is not realistic, or, c) the yield of deposited graphite is lower than our model predicts. The latter indicates that additional surface effects due to the deposition of graphite effectively harden the surface. This seems like the most likely explanation since the sputtering model for Kapton is based on measurements that were without significant contamination by graphite. This is an area for continued investigation.

Results from case b) are shown in Fig. 11 through Fig. 14. Fig. 11 shows the geometry of the geosynchronous satellite model, with surfaces broken down into triangular elements.

Results from case b) are shown in Fig. 11 through Fig. 14. Fig. 11 shows the geometry of the geosynchronous satellite

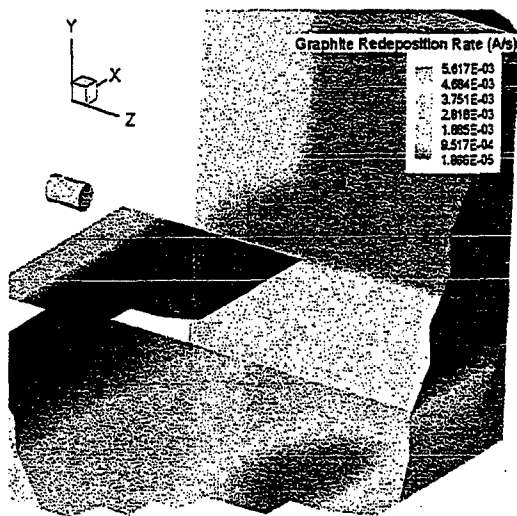


Fig. 9. Net redeposition rate of graphite (from a different viewing angle).

model. Fig. 12 shows a cross-section of a superimposed HET plume, pointing north. Plasma density is highest near the HET exhaust, and drops off rapidly as the plume expands upward toward the solar arrays.

Sputter rate was calculated using the models presented above, and is shown in Fig. 13. The total rate of redeposition of ITO from the solar array coverglass is shown in Fig. 14.

The sputtering rate peaks near the solar array corner. This illustrates a real problem with electric propulsion on geosynchronous satellites. For north-south stationkeeping, the ideal firing direction (from a thrust efficiency standpoint) is directly north. However, COLISEUM shows us that long-term firing of the HET over the lifetime of a satellite in this configuration may remove a significant amount of material from the solar array at the corner. In reality, the solar array will be rotating to track the sun, and will not always have a corner directly in the HET plume. So the configuration presented here can be considered a worst case. There are other ways of reducing the sputtering, including tilting the HET plume vector away from due north.

Redeposition of sputtered ITO, shown in Fig. 14, illustrates another potential problem in using EP onboard spacecraft. During HET firing, sputtered material from the solar panels may accumulate on the radiator panels and wings, or on other sensitive surfaces. At the rates predicted here, the emissivity of the material on top (North) of the spacecraft will almost certainly be changed, possibly affecting its ability to function properly.

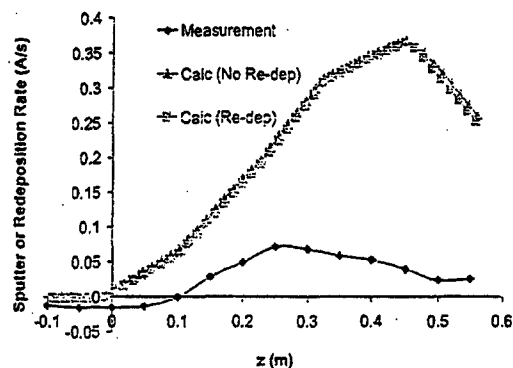


Fig. 10. Comparison between measured and calculated sputtering/redeposition rates of Kapton samples. ($x=0\text{m}$, $y=-0.188\text{m}$)

Conclusions

Although still in an early stage of development, COLISEUM now can help predict ion flux and sputtering of surface materials both onboard spacecraft and in laboratory test facilities. COLISEUM's modular architecture is allowing rapid expansion of its capabilities, and giving users flexibility to design their own geometries and choose their preferential plasma simulation method.

The model presented here for re-sputtering appears to over-predict compared to measurement. A possible cause is anomalous hardening of the surface due to deposition, in which the resulting sputter yield is greater than the original sputter yield of the deposited material.

Additional work for the future includes further investigation of the re-sputtering process and construction of new Level 1 modules that can self-consistently compute plasma expansion and interaction with surfaces.

References

- ¹Dunning, J. et al., "NASA's Electric Propulsion Program," IEPC-01-002, 27th International Electric Propulsion Conference, 2001.
- ²Spores, R. et al., "Overview of the USAF Electric Propulsion Program," IEPC-01-003, 27th International Electric Propulsion Conference, 2001.
- ³Kim, V., et al., "Electric Propulsion Activities in Russia," IEPC-01-005, 27th International Electric Propulsion Conference, 2001.
- ⁴Boyd, I. D., "A Review of Hall Thruster Plume Modeling," AIAA-00-0466, AIAA Aerospace Sciences Conference, 2000.

⁵Gardner et al., "Hall Current Thruster Plume Modeling: A Diagnostic Tool for Spacecraft Subsystem Impact," AIAA-2001-0964.

⁶Mikellides, I.G., et al., "A Hall-Effect Thruster Plume and Spacecraft Interactions Modeling Package," IEPC-01-251, 27th International Electric Propulsion Conference, 2001.

⁷Roussel et al., "Numerical Simulation of Induced Environment, Sputtering and Contamination of Satellite due to Electric Propulsion," Proc. Second European Spacecraft Propulsion Conf. 1997.

⁸K. Kannenberg, V. Khayms, S. H. Hu, B. Emgushov, L. Werthman, and J. Pollard "Validation of a Hall thruster plume sputter model," Paper AIAA-2001-3986, 37th Joint Propulsion Conference, 8-11 July 2001, Salt Lake City, Utah.

⁹V. Hruby, J. Monheiser, B. Pote, C. Freeman, and W. Connolly, "Low Power, Hall Thruster Propulsion System," IEPC-99-092, 26th International Electric Propulsion Conference, 17-21 October, 1999, Kitakyushu, Japan

¹⁰Gardner et al., "Assessment of Spacecraft Systems Integration Using the Electric Propulsion Interactions Code," AIAA-2002-3667, 38th AIAA/ASME/SAE/ASEE Joint Propulsion Conference, Indianapolis, Indiana, 2002.